

Tunable Resonant Optical MicroCavities by Self-Assembled Templating

G.V. Prakash,¹ L. Besombes,¹ T. Kelf,¹ P.N. Bartlett,² M.E. Abdelsalam,² and J.J. Baumberg¹

¹*School of Physics & Astronomy, University of Southampton, Southampton, SO17 1BJ, UK*

²*School of Chemistry, University of Southampton, Southampton, SO17 1BJ, UK*

(November 6, 2018)

Micron-scale optical cavities are produced using a combination of template sphere self-assembly and electrochemical growth. Transmission measurements of the tunable microcavities show sharp resonant modes with a Q -factor >300 , and 25-fold local enhancement of light intensity. The presence of transverse optical modes confirms the lateral confinement of photons. Calculations show sub-micron mode volumes are feasible. The small mode volume of these microcavities promises to lead to a wide range of applications in microlasers, atom optics, quantum information, biophotonics and single molecule detection.

PACS numbers:42.15.-i,07.60.Ly,81.15.Pq,42.60.Da

The operation of every type of laser, as well as many varieties of atomic traps and optical sensors, depend on the formation of an optical cavity. The resonant optical modes inside this cavity determine the spatial field distribution and spectral performance of the device. The most common optical designs use spherical mirrors to form a confocal cavity that is insensitive to misalignment and confines the optical mode to the smallest lateral dimensions. [1] The length of this cavity is on the order of the radius of curvature of the mirrors. There has been much interest in the problem of reducing the dimensions of such cavities: planar microcavities have been widely used as a way to control spontaneous emission and to enhance the interaction of light with matter, as in quantum wells [2] or quantum dots [3] but these structures only confine photons in one dimension. Confinement in lateral dimensions such as in photonic crystals [4] or microcavity mesas [5,6] can inhibit spontaneous emission altogether, but involve complex and expensive fabrication strategies. Here we present a simpler approach utilising confocal microcavities. While traditional lasers built from discrete components use macroscopic spherical mirrors, so far microcavity lasers do not. Preliminary theoretical work on the mode structure in parabolic dome [7] and spherical cavities [8] highlight the promise of such 0D microcavities, but confirm that fabrication is nontrivial. Similarly glass or polymer microspheres show high Q -factors in whispering gallery modes but it is generally hard to control them and to couple light into and out of them. [9]

To construct cavities with the smallest possible mode volume requires small radius-of-curvature mirrors. Using our recently devised route to simple fabrication of such spherical micro-mirrors, we demonstrate here the formation of stable microcavities on size-scales below 10 microns. Comparable vertical-cavity surface-emitting semiconductor lasers use planar mirror stacks integrated into the layered semiconductor growth, and then require sensitive lateral fabrication to produce small volume devices. [5,10,11] Comparable whispering gallery modes in micro-

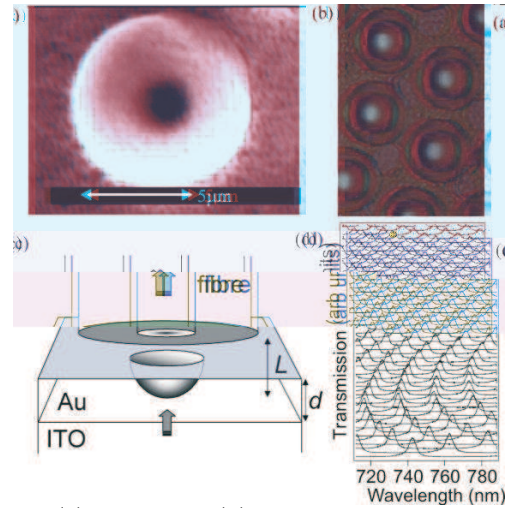


FIG. 1. (a) SEM and (b) optical micrograph of spherical micro-mirror of pore diameter $8\mu\text{m}$, radius of curvature $R=5\mu\text{m}$, in $2.5\mu\text{m}$ -thick Au on ITO. (c) Microcavity design. (d) Microcavity transmission spectra collected through the fibre for increasing separation, L , of cavity mirrors (spectra displaced vertically upwards, for each increase in cavity length $\sim 200\text{nm}$).

spheres or micro-disks have larger mode volumes and broadband tuning of the resonant cavity wavelengths is a severe problem. By robustly embedding our spherical micro-mirrors in thin metal films, we obtain simple voltage tuning by piezo-electric translation of a top planar mirror. We thus show that at length-scales approaching the wavelength of light, the electric field distribution in such microcavities can be controlled by nanoscale tuning of the mirror, and can still be interpreted using Gaussian beam optics.

Until recently, making curved mirrors in the size range required has been difficult, but advances in electrochemistry and directed self-assembly of colloidal templates now offer a cheap and simple way to produce an array of well-ordered spherical reflecting surfaces. [12] For the purposes of constructing microcavities, we combine spherical micro-mirrors of Au with radii $R < 10\mu\text{m}$ em-

bedded in a thin film, with a planar top Au mirror coated on a cleaved single-mode optical fibre. The guided mode of the fibre is then also used to efficiently couple light out of the cavity. Briefly, we use a template prepared through sedimentation of a confined colloidal solution of latex spheres on an indium-tin-oxide (ITO) coated substrate electrode to leave a self-assembled arrangement. Either close-packed arrays or isolated sphere templates can be obtained by adjusting the sphere concentration or by pre-patterning. The substrate is then placed in an electrochemical cell with a solution of aqueous metal complex ions which are deposited through reduction in the interstitial spaces of the template. The resulting film thickness can be controlled precisely through measurement of the total charge, yielding cavity shapes that range from shallow dishes to nearly-complete spherical voids. The latex spheres are removed by dissolving in tetrahydrofuran, leaving a porous metallic ‘cast’ with the ordering and size of the original template. Both electron and optical microscopy (Figs.1a,b) give an indication of the mirror quality, discussed elsewhere. [13]

By growing the micro-mirrors on semi-transparent substrates, we take advantage of the negligibly thin Au coating at the base of the mirror in order to couple light into the cavity. The results shown here use radius-of-curvature mirrors, $R=5$ and $10\mu\text{m}$ grown up to a Au thickness of around $2\mu\text{m}$ to form dish-like spherical reflectors between $5\mu\text{m}$ and $15\mu\text{m}$ across. However we have also successfully grown spherical reflectors down to $R=100\text{nm}$ radius-of-curvature. The upper cavity mirrors are formed by evaporating a 28nm thick Au film (80% reflectivity at $\lambda=750\text{nm}$) on a perpendicularly-cleaved striped single-mode optical fibre (SM660) of $100\mu\text{m}$ outer diameter, which is mounted in an XYZ piezoelectric (PZT) translation stage and aligned normally to the micro-mirror film (Fig.1c). A white-light source is focussed to a $10\mu\text{m}$ spot on the rear side of the micro-mirror film, and co-linear imaging allows us to back-illuminate individual spherical mirrors. As the fibre approaches the film, optimising the collected transmission signal brings it into correct alignment with the micro-mirror, forming the microcavity. The detected light emerging from the fibre is the product of the cavity transmission and the coupling strength to the fundamental fibre mode. Using the fibre as the top mirror thus allows a self-aligned detection geometry. We record the spectra by directly coupling the output end of the fibre to a 0.5m monochromator and CCD of combined 0.05nm resolution.

Spectral characterisation of the optical transmission through the device allows us to compare the microcavities with simple models based on Gaussian beam optics. We also produce similar 28nm -thick plane Au reflectors to directly compare our results to the plane-plane microcavity geometry using the same top fibre mirror. Typical experimental results for the transmitted modes are seen in Fig.1d, and are stable and reproducible, and similar

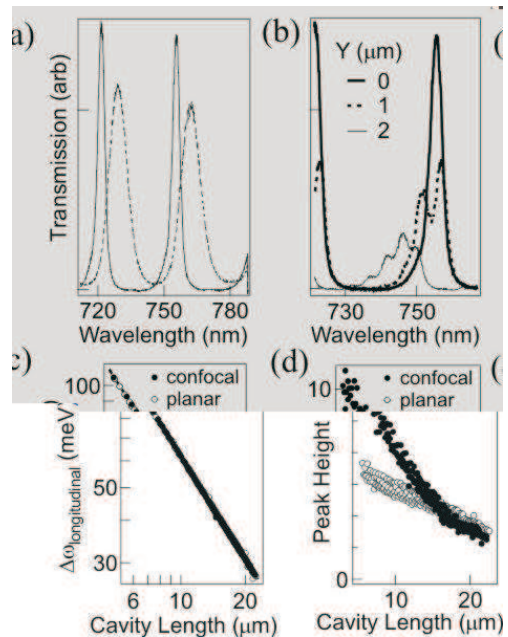


FIG. 2. Transmission spectra for cavity lengths, $L \sim 7.9\mu\text{m}$, $R=10\mu\text{m}$, for (a) plane (dashed) and confocal (solid) microcavities, and for (d) confocal microcavity with the fibre increasingly laterally shifted from the central axis ($Y=0,1,2\mu\text{m}$). (b) Longitudinal cavity mode separation for planar and confocal cavities, together with the prediction from Gaussian optics (line). (c) Peak cavity transmission as the cavity length increases.

in most well-formed spherical micro-reflectors. As expected, the spacing of longitudinal modes becomes closer together as the cavity length increases. The absolute transmission is only low here because the input coupling through the sub-micron aperture is very small for the incident incoherent white light source. Equivalent scans on a plane mirror reveal similar longitudinal modes but with a much lower finesse. A direct comparison between the plane-plane mirrors (a ‘planar’ cavity) and plane-spherical mirrors (termed ‘confocal’) is shown in Fig.2a for a cavity length, $L \sim 7.9\mu\text{m}$, with $R=10\mu\text{m}$. The general formula for the resonant frequency, ω_{npl} , that produces zero net optical phase after one round trip is given by [1]

$$\omega_{npl} = \frac{c}{L} \left\{ \pi n - \theta_{Au} + (2p + l + 1) \tan^{-1} \sqrt{\frac{L}{R - L}} \right\} \quad (1)$$

where n, p, l are positive integers describing the longitudinal, transverse radial and azimuthal mode numbers of the resonance, the second term represents the phase shift on reflection from the metal film ($\theta_{Au} \simeq 180^\circ - 24^\circ$ is the non-ideal phase shift on reflection for Au at these wavelengths), and the third term is the Gouy phase shift arising from the range of propagation angles contained in the Gaussian mode. From this paraxial approximation, the separation of the longitudinal modes yields the cavity length directly. Plotting the experimental and theoretical longitudinal mode splitting, $\Delta\omega_L$, as a function of the

cavity length derived from the calibration of the PZT Z translation gives an excellent fit for both types of cavity (Fig.2c).

The difference between the planar and confocal microcavities becomes clearer when the transmission peak heights and linewidths are compared. At cavity lengths $L < R = 10\mu\text{m}$, the finesse of the confocal microcavity approaches 10, while the quality-factor, $Q > 300$. On the other hand, the finesse of the planar microcavity does not exceed 4 due to the diffraction losses of the optical modes. This improvement can be directly seen from the peak transmission intensity vs. cavity length (Fig.2d), which is strongly enhanced for mirror separations $< R$.

To prove that the spherical mirror is acting to localise the optical modes in the transverse direction, the core of the optical fibre is laterally scanned in the XY -plane across the top opening of the spherical micro-mirror at a fixed cavity length. Typical spectra are shown in Fig.2b, and resolve a number of new optical modes. These modes always appear on the short wavelength side of the original longitudinal mode and thus can be identified as transverse modes formed by the lateral optical confinement of the spherical micro-mirror. They are never seen in plane-plane microcavities. To further study the spatial dependence of the spectral transmission, we systematically collect spectra at different X positions and plot the resulting images. Scanning across the centre of the micro-cavity (Fig.3a, $Y=0$) clearly shows the emergence of the transverse modes away from the cavity axis. The higher transverse modes dominate the spectra for scans across a chord of the circular opening (Fig.3b, $Y=2\mu\text{m}$). Up to 6 transverse modes with similar linewidths make up each longitudinal mode. Scanning in the orthogonal direction gives similar results, indicating a near-cylindrical symmetry of the micro-resonator.

These results thus allow one to directly image the different spatial mode distributions inside the microcavity, and show that the mode spectrum consists of discrete frequencies. An emitter inside a planar microcavity can always emit in some particular direction - equation (1) is valid only for normal incidence, and at different angles of incidence the resonance frequency gradually shifts to shorter wavelengths. In fundamental contrast to this behaviour, an emitter in the confocal microcavity does not have this flexibility and can only emit in the appropriate field mode, ω_{npl} . The transverse mode separation, $\Delta\omega_T$, also decreases as the cavity length increases (Fig.3c), as expected from different values of $(2p+l)$ in equation (1). However the predicted separations (Fig.3c, lines) only account reasonably for the data if the radius-of-curvature, R_{fit} , of the spherical micro-mirror is $\sim 45\mu\text{m}$ (as discussed below). Less pronounced transverse modes are also seen in $R=5\mu\text{m}$ microcavities, with similar transverse splittings, $\Delta\omega_T=12\text{meV}$ at $L=8\mu\text{m}$. The transverse spectral separation produces a corresponding lateral mode spatial separation on the order of a few hun-

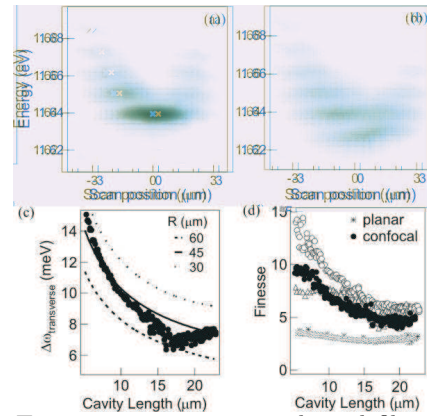


FIG. 3. Transmission spectra vs. lateral fibre X position (log scale over 1.5 decades) for (a) $Y=0$ and (b) $Y=2\mu\text{m}$, around the spectral position of a single longitudinal mode for the confocal cavity (with $R=10\mu\text{m}$) at a cavity length of $7.6\mu\text{m}$. The white crosses in (a) are predicted positions of the transverse modes collected by the fibre core. (c) Transverse mode separation vs. cavity length for $Y=1\mu\text{m}$. (d) Cavity finesse vs. cavity length for planar (\times) and confocal microcavities with one (\bullet) and two (\diamond, \triangle) transverse modes.

dred nanometres, providing a potentially effective way to couple into specific cavity modes.

The finesse of the different spectral modes is shown in Fig.3d as a function of the cavity length. Whereas the finesse of the planar structure is ~ 4 , independent of the spacing between the mirrors, the confocal microcavity performs best at small cavity separations. The maximum finesse of 15 is achieved for the lowest of the transverse modes. This agrees well with the theoretical finesse of $\pi\sqrt{r}/(1-r) \sim 14$, where $r=0.8$ is the product of the amplitude reflectivity coefficients of the two mirrors. The corresponding intensity concentrated within the cavity is $(1-r)^{-2} \sim 25$ times greater than that of the incident light at the resonant wavelength. However, as the cavity length increases beyond the mirror curvature R , the finesse drops. This is due to the increasing diameter of the transverse field profile on the spherical micro-mirror, eventually leading to it being clipped when $L > R$.

In this cylindrically symmetric micro-resonator, the field modes in the paraxial approximation are given by Laguerre-Gauss functions, [1] plotted in Fig.(4a) at the position of the top fibre mirror. This demonstrates how the microcavity dimensions here are nearly optimal to couple cavity modes into the lowest guided modes in the fibre. Higher order transverse modes have a larger diameter on the cavity mirrors hence they suffer extra loss and exhibit lower finesse, as seen in Fig.(3d). However asymmetric modes possess a field null on axis that is useful for the optical trapping of dark field species. [14]

To understand the expected spatial patterns collected by the fibre core (with its field distribution also illustrated in Fig.4a), we convolve the cavity and fibre modes to calculate the mode overlap as a function of lateral fibre position. The higher transverse modes are gener-

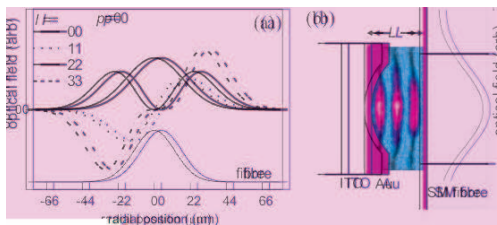


FIG. 4. (a) Optical field profiles for the fibre and the first four Laguerre-Gauss modes of the $R=10\mu\text{m}$ confocal cavity with $p=0$. (b) Calculated field distribution in a spherical confocal microcavity on resonance, $R=880\text{nm}$, $L=704\text{nm}$.

ally *not* seen for on-axial alignment due to the averaging of the oscillating electric field by the larger extent of the fibre mode. This is even more pronounced in the smaller ($R < 5\mu\text{m}$) spherical microcavities which give correspondingly smaller mode diameters. The calculated lateral offsets which optimise collection of the different transverse modes are plotted as white crosses in Fig.3a for $R=45\mu\text{m}$, giving excellent agreement with the experimental data. This concurs with the need for a larger R_{fit} that is required to account for the transverse mode spectral separation, and suggests that the spherical geometry of our micro-mirrors is imperfect. In fact, as is visible on both the micrographs of Fig.1a,b and in scanning force microscopy images (not shown), the central portion of the micro-mirrors is completely flat ($R = \infty$) where the electrochemical growth appears to be screened under the template spheres. The area of the flat region is about 10% of the total mirror area, a ratio which remains approximately the same for spherical mirrors of radius down to 100nm. Thus an effective cavity radius-of-curvature determined by both the curved and flat sections is appropriate for the theory, in accord with the experimental results. More detailed calculations based on realistic micro-mirror shapes cannot rely on the formalism for Gaussian mode propagation. However, the close match between experimental and theoretical finesse proves that this non-spherical mirror does not degrade the phase front of the lowest cavity mode, and that the mirror flatness is not a serious problem.

In $5\mu\text{m}$ radius-of-curvature cavities, the tight transverse field profiles (radius w) imply diffraction angles $\theta \simeq \lambda/\pi w > 0.50$ radians in the cavity, leading to significant errors of order 5% in the paraxial approximation, $\sin \theta = \theta$. As the size of such cavities is further reduced, these errors rapidly make conventional optical models inappropriate. Theoretical modelling to demonstrate the size scaling of these microcavities should therefore be carried out using a full solution of Maxwell's equations in these wavelength-scale geometries. The ultimate aim is to create the smallest optical cavities ($L \sim \lambda/2$) with the highest finesse. A typical electric field distribution is shown in Fig.4b for $R=880\text{nm}$, $L=704\text{nm}$, and $\lambda=750\text{nm}$ with metallic reflectors (of conductivity $200/\Omega\text{m}$ hence 80% reflectivity), corresponding to a mode volume below

$(1\mu\text{m})^3$. This shows that our templating scheme is suitable for sub-micron optical devices. For example, sub-picosecond optical modulators using resonant cavity enhancement of nonlinearities require short cavity lifetimes and hence short cavity lengths.

To summarise our key results, we have been able to fabricate near-spherical micro-mirror optical cavities with mode volumes below $(5\mu\text{m})^3$, a $Q > 300$ and finesse > 10 , and an intensity enhancement > 25 . Both longitudinal and transverse optical modes are observed, and can be simply wavelength-tuned by PZT translation of the planar top mirror which also extracts light from the cavity. In addition, this top fibre mirror can be replaced by high-reflectivity multilayers supporting luminescent nano-particles, such as semiconductor quantum dots, for enhanced emission and microlasing. The new route this opens for cavity enhancement of light-matter coupling can be further developed by reducing still further the cavity volume (we routinely produce sub-micron reflectors) and improving the finesse (using Ag or multilayer dielectric coatings), both now in progress. We note that metal mirror cavities with similar finesse have already been shown to be sufficient for attaining strong light-matter coupling in organic chromophores. [15] Our preliminary measurements already suggest that these micro-mirror cavities are useful for optical-dipole force trapping, for enhanced collection of micro-photoluminescence from the focal region, or for incorporation in experiments involving cold atom interactions on integrated chips.

We gratefully thank Ed Hinds and Tim Fregarde for helpful discussions of resonator design, and Oliver Wright and Dave Hanna for critical comments. We acknowledge financial support from JSPS, EPSRC GR/N37261, GR/R54194, GR/S02662 and GR/N18598.

-
- [1] A.E. Seigman, *Lasers* (University Science Books, Mill Valley, Calif., 1986).
 - [2] G. Khitrova *et al.*, *Rev. Mod. Phys.* **71**, 1591 (1999).
 - [3] H. Saito, K. Nishi, I. Ogura, S. Sugou, Y. Sugimoto, *Appl. Phys. Lett.* **69**, 3140 (1996).
 - [4] E. Yablonovitch, *Phys. Rev. Lett.* **58**, 2059 (1987).
 - [5] J.M. Gerard *et al.*, *Appl. Phys. Lett.* **69**, 449 (1996).
 - [6] J.M. Gerard, B. Gayral, *J. Lightwave Technol.* **17**, 2089 (1999).
 - [7] J. Nockel *et al.*, *Phys. Rev.* **E62**, 8677 (2000).
 - [8] R.A. Abram, S. Brand, M.A. Kaliteevski, V.V. Nikolaev, *Phys. Stat. Sol.* **183**, 183 (2001).
 - [9] R. Jia, D-S. Jiang, P-H. Tan, B-Q Sun, *Appl. Phys. Lett.* **79**, 153 (2001).
 - [10] J.L. Jewell *et al.*, *Electron. Lett.* **25**, 1123 (1989).
 - [11] K.L. Lear, E.D. Jones, *MRS Bull.* **27**, 497 (2002).
 - [12] P.N. Bartlett, P.R. Birkin, M.A. Ghanem, *Chem. Commun.*, 1671 (2000).
 - [13] S. Coyle, G.V. Prakash, J.J. Baumberg, M. Abdelsalam, P.N. Bartlett, *Appl. Phys. Lett.* **83**, 767 (2003).
 - [14] M. P. MacDonald *et al.*, *Science* **296**, 1101 (2002).
 - [15] P.A. Hobson *et al.*, *Appl. Phys. Lett.* **81**, 3519 (2002).